

Uncalibrated Visual Odometry for Ground Plane Motion Without Auto-calibration

Vincenzo Caglioti¹ and Simone Gasparini¹

Politecnico di Milano - Dipartimento di Elettronica e Informazione
Piazza Leonardo da Vinci, 32 - I-20133 Milano (MI), Italy

Abstract. In this paper we present a technique for visual odometry on the ground plane, based on a single, uncalibrated fixed camera mounted on a mobile robot. The odometric estimate is based on the observation of features (e.g., salient points) on the floor by means of the camera mounted on the mobile robot. The presented odometric technique produces an estimate of the transformation between the ground plane prior to a displacement and the ground plane after the displacement. In addition, the technique estimates the homographic transformation between ground plane and image plane: this allows to determine the 2D structure of the observed features on the ground. A method to estimate both transformations from the extracted points of two images is presented. Preliminary experimental activities show the effectiveness and the accuracy of the proposed method which is able to handle both relatively large and small rotational displacements.

1 Introduction

Robot localization is a fundamental process in mobile robotics application. One way to determine the displacements and measure the movement of a mobile robot is dead reckoning systems. However these systems are not reliable since they provide noisy measurements, due to the slippage of the wheel. Localization methods based only on dead reckoning have been proved to diverge after few steps [1]. Visual odometry, i.e. methods based on visual estimation of the motion through images capture by one or more cameras, is exploited to obtain more reliable estimates. Cameras are mounted on the robot and the images are processed in order to recover the structure of the surrounding environment and estimate the motion among images captured from different viewpoints.

Usually, 3D reconstruction from images taken by a moving uncalibrated camera go through auto-calibration. Autocalibration from planar scenes requires either nonplanar motion [2], or several planar motions with different attitudes of the camera wrt the ground plane [3].

In a mobile robotics framework, however, changing camera attitude requires additional devices as, e.g., pan-tilt heads, not directly connected to the robot functionality. In particular, mounting a fixed monocular camera on a mobile robot does not allow to change the camera attitude wrt to the ground plane, making auto-calibration impossible

without additional information. A similar scenario is that of a fixed camera mounted on a moving vehicle (such as, e.g., a road car).

However, in this paper we will present a technique for visual odometry on the ground plane, based on a single, uncalibrated fixed camera mounted on a mobile robot. The mobile robot is supposed to move on a planar floor, called ground plane. No map of the environment is needed. The odometric estimate is based on the observation of features (e.g., salient points) on the floor by means of the camera mounted on the mobile robot.

The presented odometric technique produces an estimate of the transformation between the ground plane prior to a displacement and the ground plane after the displacement. In addition, the technique estimates the homographic transformation between ground plane and image plane: this allows to determine the 2D structure of the observed features on the ground, as a side effect. The presented technique does not determine the camera calibration parameters.

However, it is argued that any further step towards auto-calibration is not needed in the context of mobile robot odometry. In fact, auto-calibration would only allow to determine the spatial transformation between ground plane and camera: auto-calibration alone does not allow to determine the robot-to-camera transformation. Therefore, determining the transformation between the robot and the ground plane should require further extrinsic calibration steps: these steps could consist in e.g., acquiring visual data while the robot is executing self-referred displacements (such as, a self-rotation and a forward translation).

On the other hand, the presented technique for visual odometry estimates the transformation between ground prior to a displacement and ground after the displacement. If needed, the robot-to-ground calibration can be accomplished by the same additional step, namely visual observation of self-referred robot displacements, required when starting with auto-calibration.

The technique works for generic planar displacements, but it does not work for translational displacements. However, once the homography between ground plane and image plane has been determined as a side effect, further displacements, including pure translations, can be analyzed directly by using the (inverse) homography.

1.1 Related Works

In the last years methods to estimate the robot motion (ego-motion) based on visual information provided by cameras have gained attention and some approaches have been presented. Early methods were based on estimation of the optical flow from image sequence in order to retrieve ego-motion. McCarthy and Barnes [4] presented a review and a comparison between the most promising methods.

Other approaches exploited stereo vision. Nister et al. [5] proposed a method based on triangulation between stereo pairs and feature tracking in time-sequence of stereo pairs, without any prior knowledge or assumption about the motion and the environment. Takaoka et al. [6] developed a visual odometry system for a humanoid robot based on feature tracking and depth estimate using stereo pairs. Agrawal and Konolige [7] proposed an integrated, real-time system involving both stereo estimate in the disparity space and a GPS sensor in a Kalman filter framework. GPS-based systems can be

sufficiently accurate for large areas but it can be not used in indoor environments and require a support framework, which prevent their use, e.g., for planetary exploration. For such application, Mars Exploration Rover [8] employed a features detection in a stereo image pair that are tracked from one frame to the next; using maximum likelihood estimation the change in position and attitude for two or more pairs of stereo images is determined.

Davison [9] proposed a real-time framework for ego-motion estimation for a single camera moving through general unknown environments. The method was based on a Bayesian framework that detect and track a set of features (usually corner, points or lines). Assuming the rigidity in the scene, the feature image motion allows to estimate the motion of the camera; therefore the complete camera trajectory and a 3D map of all the observed features can be recovered.

Visual odometry system based on catadioptric cameras have been proposed. Bunschoten and Krose [10] used a central catadioptric camera to estimated the relative pose relationship from corresponding points in two panoramic images via the epipolar geometry; the scale of the movement is subsequently estimated via the homography relating planar perspective images of the ground plane. Corke et al. [11] developed a visual odometry system for planetary rover based on a catadioptric camera; they proposed a method based on robust optical flow estimate from salient visual features tracked between pairs of images, by which they retrieve the displacements of the robot.

Our approach is similar in spirit to the work of Wang et al. [12] who measured translation and rotation by detecting and tracking features in image sequences; assuming that the robot is moving on a plane, they computed the homography between the image sequences by which the computed the motion. Similarly, Benhimane and Malis [13] developed a visual servoing framework based on the estimation of the homography between image sequences to retrieve robot motion and close the control loop. Both methods require camera calibration. Our work differ from these approaches in that we do not assume camera calibration.

The paper is structured as it follows. Section 2 introduces and describes the addressed problem. Section 3 shows how the robot displacement can be retrieved by fitting the homography between two images of the ground plane. Section 4 illustrates the method to estimate the transformation between the ground plane and the image plane. Section 5 reports and discussed some preliminary experimental activities performed with a rotating camera. Section 6 concludes the paper.

2 Problem Formulation

A mobile robot moves on the floor. A fixed, uncalibrated camera is mounted on the mobile robot: this camera is supposed to be a perspective camera (i.e., distortion is neglected). The pose of the camera relative to the robot is unknown. The environment map is unknown, as well as the structure of the observable features (associated to floor texture) on the ground. This allows extremely easy set-up: it is sufficient to mount a perspective camera on the mobile robot in a fixed but unknown position.

For the rigid body consisting of the robot plus the camera, a “ground” reference frame is defined as follows: the backprojection O of a certain image pixel (say, the pixel

O' with cartesian coordinates $(0,0)$) on the ground plane is taken as the origin of the projected reference frame, while vector connecting the origin to the backprojection A of a second image pixel (say, the pixel A' with cartesian coordinates $(100,0)$) on the ground is taken as the unit vector along the x -axis.

As usual within the Robotics and Vision communities, homogeneous coordinates are used. Let T be the unknown 3×3 matrix representing the projective transformation, also called “homography”, between the ground plane and the image plane, as realized by the uncalibrated camera. The coordinates on the ground plane are referred to the above defined ground reference frame of the robot+camera system. Therefore, the unknown homography T does not change with robot motion.

As the robot moves on the ground plane, the robot+camera undergoes a planar motion consisting of a rotation of an unknown angle θ about an unknown vertical axis. Let C be the point where this vertical axis crosses the horizontal ground plane. Let R be the rotation matrix describing the planar displacement. The matrix R is a 3×3 2D rotation matrix in homogeneous coordinates, whose third column collects the homogeneous coordinates of the center of rotation C relative to the robot+camera ground reference and whose upper-left 2×2 sub-matrix is orthogonal.

Two images are taken: the first one is taken before the displacement, while the second one is taken after the displacement. The addressed problem is the following: first, given the transformation between the first and the second image, determine the center of rotation, and the rotation angle of the observed displacement; second, determine the transformation T between the ground plane and the image plane, and use the inverse transformation T^{-1} to measure further displacements. The inverse transformation T^{-1} can also be used to determine the shape (i.e., the 2D structure) of the set of the observed features on the ground.

An interesting problem, which is not addressed in this paper, is that of finding a transformation between the ground robot+camera reference frame and a second reference frame, more significant to the robot kinematics. This transformation can be estimated by applying the presented odometric technique to self-referred robot displacement, as e.g., a “self”-rotation and a “forward” translation.

3 Estimation of Robot Displacement

The transformation relating the two images of the ground plane is still a homography, and it is represented by the matrix $H = TRT^{-1}$, where T is the unknown homography between ground plane and image plane. (In principle, camera distortion can be compensated by imposing that the transformation between the two images is a homography.)

The homography H between the two images (before and after the displacement) can be computed from a sufficient number of pairs of corresponding features between the two images [14].

The eigenvectors of the homography matrix H are given by $C' = TC$, $I' = TI$ and $J' = TJ$, where the rotation center C , and the circular points I and J are the invariants under rotation R on the ground plane. In addition, the eigenvalues of H coincide with the eigenvalues of R (modulo a scale factor).

The eigenvector C' is associated to the real eigenvalue of H , while I' and J' are associated to the complex eigenvalues of H . By the eigendecomposition of the homography matrix H , the parameters of the planar displacement are determined.

In particular, the image C' of the center of rotation C is determined as the eigenvector corresponding to the real eigenvalue of H . The rotation angle θ is determined as the ratio between imaginary part and real part of the complex eigenvalue, in fact the eigenvalue corresponding to $I' = TI$ is given by $\mu e^{\pm i\theta}$, where μ is a real scale factor.

If the displacement is a pure translation, then the images of all the points at the infinity are eigenvectors of H . Therefore the translation direction can not be determined. Therefore, displacements with small rotation angles may generate solutions, that are numerically unstable.

4 Estimation of the Transformation Between the Ground Plane and the Image Plane

The shape of the observed features is determined by estimating the transformation matrix T . This matrix can be estimated by four pairs of corresponding points: these can be, e.g., the two circular points $I = [1, i, 0]^T$, $J = [1, -i, 0]^T$ with their image projections I' , J' , plus the two points defining the robot+camera ground reference, namely $O = [0, 0, 1]^T$ and $A = [1, 0, 1]^T$, with their image projections $O' = [0, 0, 1]^T$ and $A' = [100, 0, 1]^T$.

The homogeneous (world) coordinates of O within the ground reference are $[0, 0, 1]$ while the homogeneous coordinates of A within the ground plane are $[1, 0, 1]$. With these choices, the transformation matrix T between ground plane and image plane is fully constrained, and it can be determined, imposing that

$$\begin{cases} I' = TI \\ J' = TJ \\ O' = TO \\ A' = TA \end{cases}$$

Once the transformation matrix T has been estimated, the shape of any configuration of observed features can be determined by their images ($P'_i, i = 1..n$) by $P_i = T^{-1}P'_i$. The knowledge of T allows to determine the coordinates of the rotation center $C = T^{-1}C'$ relative to the (back-projected) robot reference. The estimated motion parameters constitute an odometric estimate of the robot displacement.

Notice that the shape determination requires that the displacement is not purely translational. However, once the transformation T has been determined by analyzing a rotational displacement, it can be used also to measure purely translational displacements.

5 Preliminary Experimental Results

In order to validate the proposed method we performed some experimental activities.

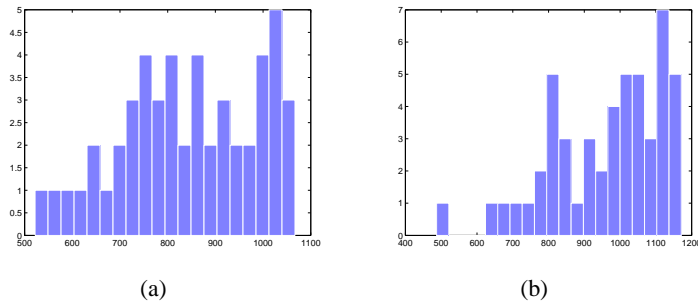


Fig. 1. The distribution of the matching score of the features used to estimate $\theta_{5,6}$ (a) and $\theta_{6,7}$ (b).

Table 1. The first sequence of 7 images taken with relatively large rotational displacements. The table reports the ground truth references (θ_{ref} , in degrees) read on the turntable, the rotational displacements between two consecutive images ($\theta_{i,i+1}$), the estimated rotational angles ($\hat{\theta}_{i,i+1}$) and the relevant error ($e_{\hat{\theta}_{i,i+1}}$). The value of $\theta_{6,7}$ was obtained with a lower number of features ($N = 10$) since many outliers were found.

Step	θ_{ref}	$\theta_{i,i+1}$	$\hat{\theta}_{i,i+1}$	$e_{\hat{\theta}_{i,i+1}}$
1	107	9	9.37	-0.37
2	116	8.5	8.09	0.41
3	124.5	10.5	10.35	0.15
4	135	8	7.91	0.09
5	143	11	10.97	0.03
6	154	10.5	9.70	0.8

In our experimentations we use a standard perspective camera provided with a very low distortion optics. The camera was placed on a turntable by which we manually measured the ground truth rotation with an accuracy of about 0.5° . The camera viewpoint was placed in a generic position relative to the rotation axis: therefore the camera underwent a general planar motion. The camera was pointed towards the ground floor, such that the extraction of salient points exploits the floor texture. Then we took some images with different rotational displacement and applied the proposed method in order to estimate the rotation angle between two images.

We tested the method on two sequences of images. The first sequence was obtained considering larger rotational displacements, with a mean angle of about 10° . The second sequence is characterized by relatively small rotational displacements between images. The mean rotational displacement of this set is about 5° . As discussed in Section 3, small rotation angles may lead to numerical instability. On the other hand if the robot rotates slowly, images with small rotational displacements have to be taken into account.

Table 1 collects the ground truth values, the estimated values and the relevant errors for the first sequence. For this sequence we employed the following estimation procedure. Given two consecutive images, say I_i and I_{i+1} , we extracted a number of salient

Table 2. The second sequence of 25 images taken with relatively small rotational displacements. For each step, the table reports the ground truth references (θ_{ref} , in degrees) read on the turntable, the relative rotational displacements among the three consecutive images ($\theta_{i,i+1}$ and $\theta_{i,i+2}$), the estimated rotational angles ($\hat{\theta}_{i,i+1}$) and the relevant error ($e_{\hat{\theta}_{i,i+1}}$).

Step	θ_{ref}	$\theta_{i,i+2}$	$\theta_{i,i+1}$	$\theta_{i+1,i+2}$	$\hat{\theta}_{i,i+2}$	$e_{\hat{\theta}_{i,i+2}}$
1	321	12	7	5	11.83	0.17
2	314	12	5	7	12.16	-0.16
3	309	8.5	7	1.5	7.83	0.67
4	302	10	1.5	8.5	10.81	-0.81
5	300.5	14	8.5	5.5	7.97	6.03
6	292	10	5.5	4.5	9.25	0.75
7	286.5	7.5	4.5	3	7.03	0.47
8	282	10	3	7	9.36	0.64
9	279	12	7	5	11.58	0.42
10	272	10.5	5	5.5	9.93	0.57
11	267	9.5	5.5	4	8.70	0.80
12	261.5	10.5	4	6.5	9.96	0.54
13	257.5	10.5	6.5	4	10.02	0.48
14	251	9	4	5	8.71	0.29
15	247	7	5	2	7.50	-0.50
16	242	8	2	6	7.01	0.99
17	240	10	6	4	9.03	0.97
18	234	10.5	4	6.5	10.78	-0.28
19	230	10	6.5	3.5	9.52	0.48
20	223.5	10	3.5	6.5	10.91	-0.91
21	220	10	6.5	3.5	10.72	-0.72
22	213.5	7.5	3.5	4	7.21	0.29
23	210	8.5	4	4.5	8.96	-0.46

points from each image using the Harris features extractor [15]. Then we found the correspondences among these points using the normalized cross correlation and we selected a set of points (usually, $N = 20$) having the best matching score [16]. We used this set of points to fit the homography $H_{i,i+1}$ using the RANSAC technique [17] provided by [18]. Once $H_{i,i+1}$ was computed, we estimated the rotation angles from the complex eigenvalues of $H_{i,i+1}$, as explained in Section 3.

As Table 1 shows, the estimates are very accurate and the errors are less than 1° . The value of $\theta_{6,7}$ was obtained considering a lower number of salient point, $N = 10$. Because of the large rotational displacement (about 10.5°) the matching among features was in most cases incorrect and the resulting matching score was (on the average) higher with respect to the other images of the sequence. Figure 1 compares the distributions of the matching score values of the first 50 best matches for image pairs used to compute c and $\theta_{6,7}$ respectively: the estimation process of $\theta_{5,6}$ can rely on many reliable matching features (e.g. at least 20 matches have a matching score less than 800) while for the estimation process of $\theta_{6,7}$ there are only few matches under the same threshold. This introduced many outliers that affected the estimate. Decreasing the number of considered points allowed to discard many outliers, thus obtaining a more reliable estimate.

Table 2 collects the ground truth values, the estimated values and the relevant errors for the second sequence. In order to overcome possible numerical instability issues we used three images to robustly estimate the angle. We employed the following estimation procedure. Given three consecutive images, say I_i , I_{i+1} and I_{i+2} , we extracted a number of salient points from each image, say c_i , c_{i+1} and c_{i+2} respectively. We found the

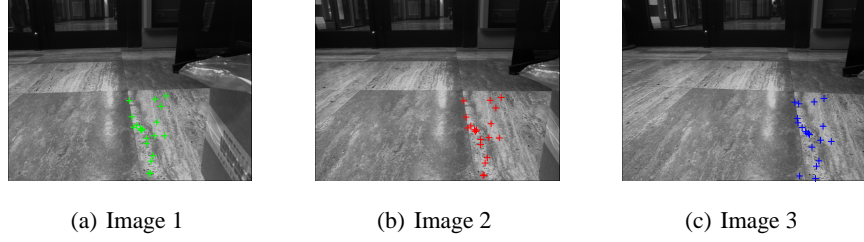


Fig. 2. An example of tracked features between three images. The first two images (a,b) are compared in order to find the best matches (depicted in green and red, respectively). The best features of (b) are matched with (c) in order to find the best matches (depicted in blue in (c)). Hence the chain of matches between the images are used to computed the homography $H_{i,i+2}$.

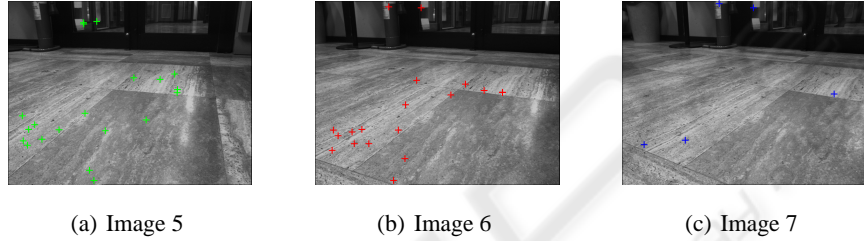


Fig. 3. The images (from 5 to 7) of the second sequence for which the estimated rotation angle was incorrect. The found corresponding features among images are depicted: most of the matches are false matches, which led to an incorrect estimation of the homography $H_{5,7}$.

correspondences among the features c_i and c_{i+1} , selecting only those matches having the best matching score, say c'_i and c'_{i+1} . Then we tracked these matches in I_{i+2} by matching c'_{i+1} with the features c_{i+2} , selecting the best matches and obtaining c''_{i+1} and c''_{i+2} (where $c''_{i+1} \subseteq c'_{i+1}$).

Exploiting c''_{i+1} , we also obtained c''_i , which are features of I_i that have a matching feature both in I_{i+1} and I_{i+2} . By fitting a homography with c''_i and c''_{i+2} , we computed the 3×3 matrix $H_{i,i+2}$ with the RANSAC technique, obtaining the relevant rotation angle $\theta_{i,i+2}$. Figure 2 shows an example of the tracked features among the three images.

The reported results proved the effectiveness and the accuracy of the proposed method. The estimation errors are less than 1° , except for images 5, 6 and 7. In this case the errors is greater since the method was not able to find a correct rotational angle. This is due to the large displacements among images: the overall displacement between image 5 and 7 is about 14° , with partial displacements of 8.5° and 5.5° respectively. Figure 3 shows the matching feature that are used to determine the rotational displacements: there are many false matching that affected the estimate of $\theta_{5,7}$.

Large displacements may cause such errors since we used the normalized cross correlation to find the correspondences. Normalized cross correlation is not rotationally invariant, hence large rotation can corrupt the matching process. Moreover, large rota-

tion angles between images reduce the overlapping region of the images, thus reducing the number of corresponding features. In order to overcome these issues, rotationally invariant matching function can be employed such as, e.g., SIFT features extractor [19]. On the other hand, in a real application a proper visual sampling rate during robot movement would avoid large displacements between two poses.

6 Conclusions and Ongoing Activity

In this paper we presented a novel method to estimate the odometry of a mobile robot through a single uncalibrated fixed camera. Assuming that the robot is moving on a planar floor, images of the floor texture is taken. Salient points are extracted from the image and are used to estimate the transformation between the ground plane before a displacement and the ground plane after the displacement. The proposed technique also estimate the homography between the ground plane and the image plane, which allows to determine the 2D structure of the observed features. An estimation method of both transformations was described. Preliminary experimental activities that validate the method for small and large rotational displacements are also presented and discussed.

Ongoing works are aimed at improving the estimate method in order to provide reliable estimate in presence of large rotational displacements. Other experimental activities will be conducted in order to better stress the method in different situations. We are also planning to implement a real time version of the proposed method on a real application in order to use the odometric estimate for localization tasks in a mobile robots. Other possible future research direction are the employment of catadioptric cameras in order to exploit their large field; however, using catadioptric cameras the transformations are not homography, unless central catadioptric cameras are used, which are, on the other hand, difficult to set up.

References

1. Borenstein, J., Feng, L.: Measurement and correction of systematic odometry errors in mobile robots. *IEEE Transaction on Robotics and Automation* **12** (1996) 869–880
2. Triggs, B.: Autocalibration from planar scenes. In: *Proceedings of the European Conference on Computer Vision (ECCV '98)*, London, UK, Springer-Verlag (1998) 89–105
3. Knight, J., Zisserman, A., Reid, I.: Linear auto-calibration for ground plane motion. In: *Proceedings of the IEEE International Conference on Computer Vision and Pattern Recognition (CVPR '03)*. Volume 1., Los Alamitos, CA, USA, IEEE Computer Society (2003) 503–510
4. McCarthy, C., Barnes, N.: Performance of optical flow techniques for indoor navigation with a mobile robot. In: *Proceedings of the IEEE International Conference on Robotics and Automation*. Volume 5., Los Alamitos, CA, USA, IEEE Computer Society (2004) 5093–5098
5. Nister, D., Naroditsky, O., Bergen, J.: Visual odometry. In: *Proceedings of the IEEE International Conference on Computer Vision and Pattern Recognition (CVPR '04)*. Volume 1., Los Alamitos, CA, USA, IEEE Computer Society (2004) 652–659
6. Takaoka, Y., Kida, Y., Kagami, S., Mizoguchi, H., Kanade, T.: 3d map building for a humanoid robot by using visual odometry. In: *Proceedings IEEE International Conference*

- on Systems, Man, and Cybernetics. Volume 5., Los Alamitos, CA, USA, IEEE Computer Society (2004) 4444–4449
7. Agrawal, M., Konolige, K.: Real-time localization in outdoor environments using stereo vision and inexpensive gps. In: Proceedings of the International Conference on Pattern Recognition (ICPR '06). Volume 3., Los Alamitos, CA, USA, IEEE Computer Society (2006) 1063–1068
 8. Cheng, Y., Maimone, M., Matthies, L.: Visual odometry on the mars exploration rovers - a tool to ensure accurate driving and science imaging. IEEE Robotics and Automation Magazine **13** (2006) 54–62
 9. Davison, A.: Real-time simultaneous localization and mapping with a single camera. In: Proceedings of the IEEE International Conference on Computer Vision (ICCV '03), Los Alamitos, CA, USA, IEEE Computer Society (2003) 1403–1410
 10. Bunschoten, R., Krose, B.: Visual odometry from an omnidirectional vision system. In: Proceedings of the IEEE International Conference on Robotics and Automation. Volume 1., Los Alamitos, CA, USA, IEEE Computer Society (2003) 577–583
 11. Corke, P., Strelow, D., Singh, S.: Omnidirectional visual odometry for a planetary rover. In: Proceedings of the IEEE/RSJ International Conference on Intelligent Robots and Systems. Volume 4., Los Alamitos, CA, USA, IEEE Computer Society (2004) 4007–4012
 12. Wang, H., Yuan, K., Zou, W., Zhou, Q.: Visual odometry based on locally planar ground assumption. In: Proceedings of the IEEE International Conference on Information Acquisition. (2005) 6pp.
 13. Benhimane, S., Malis, E.: Homography-based 2d visual servoing. In: Proceedings of the IEEE International Conference on Robotics and Automation, Los Alamitos, CA, USA, IEEE Computer Society (2006) 2397–2402
 14. Hartley, R.I., Zisserman, A.: Multiple View Geometry in Computer Vision. Second edn. Cambridge University Press (2004)
 15. Harris, C., Stephens, M.: A combined corner and edge detector. In: Proceedings of the Fourth Alvey Vision Conference. (1988) 147–152
 16. Torr, P.H.S., Murray, D.W.: Outlier detection and motion segmentation. In Schenker, P.S., ed.: Sensor Fusion VI, SPIE volume 2059 (1993) 432–443 Boston.
 17. Fischler, M.A., Bolles, R.C.: Random sample consensus: a paradigm for model fitting with applications to image analysis and automated cartography. Communication of ACM **24** (1981) 381–395
 18. Kovesi, P.D.: MATLAB and Octave functions for computer vision and image processing. School of Computer Science & Software Engineering, The University of Western Australia (2004) Available from: <http://www.csse.uwa.edu.au/~pk/research/matlabfns/>.
 19. Lowe, D.G.: Distinctive image features from scale-invariant keypoints. International Journal of Computer Vision **60** (2004) 91–110